

Article

Optimization of the Conditions for the Transformation of a *Bacillus subtilis* Strain L11 to Prepare Nano Selenium and Its Preliminary Application in Sheep Feed

Wenxin Guo ^{1,2}, Xinyu Shi ^{1,2}, Lu Wang ^{1,2}, Xin Cong ^{1,2}, Shuiyuan Cheng ^{1,2}, Linling Li ^{1,2,*} and Hua Cheng ^{1,2,*} 

¹ School of Modern Industry for Selenium Science and Engineering, Wuhan Polytechnic University, Wuhan 430048, China; gwxxwhpu1012@163.com (W.G.); sxy549144862@126.com (X.S.); m15656753051@163.com (L.W.); 13905189777@163.com (X.C.); 12316@whpu.edu.cn (S.C.)

² National R & D Center for Se-Rich Agricultural Products Processing, Wuhan Polytechnic University, Wuhan 430023, China

* Correspondence: 12622@whpu.edu.cn (L.L.); 12621@whpu.edu.cn (H.C.); Tel.: +86-173-7156-9920 (H.C.)

Abstract: Selenium nanoparticles (SeNPs) have greater bioavailability and safety than inorganic selenium, and was widely used in medical, agricultural, nutritional supplements, and antibacterial fields. The present study screened a strain L11 producing SeNPs from a selenium rich dairy cow breeding base in Hubei Province, China. The strain was identified as *Bacillus subtilis* through physiological, biochemical, and molecular biology analysis. By adjusting the cultivation conditions, the experiment determined the ideal parameters for L11 to efficiently produce SeNPs. These parameters include a pH value of 6, a cultivation temperature of 37 °C, a concentration of 4 mmol/L Na₂SeO₃, and a cultivation of 48 h. X-ray Photoelectron Spectroscopy (XPS), Scanning Electron Microscope-Energy Dispersive Spectroscopy (SEM-EDS), and Transmission Electron Microscopy (TEM) were used to verify that the Se particles produced by L11 are SeNPs with diameters ranging from 50 to 200 nm. The combination of the protein analysis of different cell components and TEM analysis showed that L11 mainly produces SeNPs through the transformation of the cell's periplasmic space, cell membrane, and cell wall. Adding the L11 SeNPs complex to sheep feed can significantly enhance the antioxidant activity and immunity of sheep, and increase the Se content in the neck muscles, liver, and spleen tissues.

Keywords: *Bacillus subtilis*; SeNPs; subcellular localization; biological activity; immunity



Citation: Guo, W.; Shi, X.; Wang, L.; Cong, X.; Cheng, S.; Li, L.; Cheng, H. Optimization of the Conditions for the Transformation of a *Bacillus subtilis* Strain L11 to Prepare Nano Selenium and Its Preliminary Application in Sheep Feed. *Microbiol. Res.* **2024**, *15*, 326–341. <https://doi.org/10.3390/microbiolres15010022>

Academic Editor: Juan Ayala

Received: 16 January 2024

Revised: 20 February 2024

Accepted: 24 February 2024

Published: 26 February 2024



Copyright: © 2024 by the authors. Licensee MDPI, Basel, Switzerland. This article is an open access article distributed under the terms and conditions of the Creative Commons Attribution (CC BY) license (<https://creativecommons.org/licenses/by/4.0/>).

1. Introduction

Selenium (Se) was a metalloid element discovered by a Swedish chemist Jacob Berzelius in 1818. Its name comes from the Greek meaning of “Selene” for the goddess of the moon [1]. Se was considered an essential element for plants and mammals. This non-metallic element plays an important role in improving human function and preventing cell damage by producing selenoprotein [2]. Se compounds also participate in the neutralization of heavy metals by directly or indirectly binding to ions, preventing them from causing damage to healthy cells [3]. The inorganic states of Se commonly present in nature include selenides (Se²⁻), selenite (SeO₃²⁻), and selenate (SeO₄²⁻), and its two main organic forms are seleno-cysteine (SeCys) and selenomethylamine (SeMet), which form various Se proteins. In a reducing environment, the oxygen anion of Se is converted into a typical red elemental state, which significantly reduces its toxicity. The elemental form can be further reduced to organic selenides [1,4]. Although Se is essential to the human body, on the other hand, excessive intake can increase its accumulation in tissues and exhibit toxicity. Because its inorganic ions in tissues can cause oxidative stress, organic components such as SeCys or SeMet may be mismatched during translation, leading to disordered protein synthesis [5].

The margin between Se deficiency and toxicity is very thin. The ideal intake of Se recommended by the World Health Organization in 2009 was 50–55 µg per day in a human

diet based on individual weight [6]. Some reports also indicated that the minimum intake of dietary Se was 55 µg per day and the maximum limit was 400 µg. Excessive intake of Se by adults can lead to severe Se poisoning [1]. Se oxide anions are the most active form of Se in nature, which are easily ingested by animals and humans from contaminated water streams, and even indirectly ingested by plants irrigated with Se-rich water, leading to many health hazards [7]. On the contrary, Selenium nanoparticles (SeNPs) exhibit high biological activity and adsorption potential due to their interactions with protein chemical groups. Therefore, SeNPs were widely used in medical diagnosis, dietary supplements, cancer treatment, and environmental biotechnology [8,9]. SeNPs can be generated through chemical, physical, or biological methods, and their physicochemical properties depend on the conversion method [10]. The use of physical and chemical methods to produce nanoparticles releases toxic and dangerous chemicals, which have low biocompatibility and limit their application [11]. From previous research results, it can be seen that synthesizing SeNPs using biological methods is safe, inexpensive, and simple. *B. subtilis* is a probiotic that does not pose any environmental safety risks during the Se (IV) reduction process. According to reports, this bacterium can convert Se into SeNPs by inducing detoxification systems rather than alienating the electron transfer [11,12].

Se, an essential trace element in the human body, holds a profound relationship with human health and disease etiology. Organic Se exhibited superior bioavailability and safety compared to inorganic Se, and SeNPs possess advantageous toxicological and reactive properties over other organic Se forms. In this study, a Se-rich probiotic was screened and isolated from fermented mature forage samples collected from a Se-enrich dairy cow breeding base in Hong'an County, Hubei Province. This isolation was achieved through a combination of high-concentration Na₂SeO₃ stress and confrontation culture with pathogenic microorganisms. One Se rich *B. subtilis* strain was screened by combining the morphology, physiology, biochemistry, and 16S rDNA sequence analysis. This study aimed to optimize the growth conditions for the biosynthesis of SeNPs by modified *Bacillus* species. The characterization and analysis of the produced SeNPs were conducted using X-ray Photoelectron Spectroscopy (XPS), Scanning Electron Microscope-Energy Dispersive Spectroscopy (SEM-EDS), and Transmission Electron Microscopy (TEM) techniques. Additionally, *B. subtilis* harboring SeNPs were incorporated into sheep feed as probiotics to preliminarily investigate their effects on physiological and biochemical indicators as well as Se content in different sheep tissues.

2. Materials and Methods

2.1. Bacterial Strains and Culture Medium

Se-rich probiotics were isolated from forage samples from the Se-rich dairy cow breeding base in Hong'an County (latitude 31°13' N, longitude 114°48' E), Hubei Province, China, using dual screening of high-concentration Na₂SeO₃ stress and pathogenic microbial confrontation culture. And, combined with morphology, physiology, biochemistry, and 16S rDNA sequence to identify Se rich probiotic strain L11. LB medium: Tryptone 10 g/L, yeast extract 5 g/L, sodium chloride 10g/L, adjust the pH of the medium to 7.2. *B. subtilis* universal culture medium as follows: 20 g/L glucose, 15 g/L peptone, 5 g/L NaCl, 0.5 g/L beef extract. Na₂SeO₃ was purchased from Sigma (Darmstadt, Germany) in the experiment.

The original *Bacillus subtilis* strain L11 was inoculated into 100 mL of LB medium in a triangular flask and incubated at 37 °C with shaking at 180 rpm. The cell concentration was determined using a visible spectrophotometer at 600 nm (OD₆₀₀), and the culture was grown until the OD₆₀₀ reached 1.0. Then, 1 mL of the activated bacterial suspension was transferred into 100 mL of fresh LB medium and *B. subtilis* general medium, respectively. Both cultures were incubated at 37 °C with shaking at 180 rpm for 48 h. Samples were taken every 2 h to measure the OD₆₀₀ value of the bacterial suspension. Three replicates were set up for each condition, and growth curves were plotted for the *Bacillus subtilis* strain L11 in both media (Table S1).

2.2. Identification of Se-Tolerant Strains

To assess the colony morphology of strain L11, the bacterium was cultured on LB agar plates for 48 h. Subsequently, crystal violet staining was applied to the strain, followed by microscopic examination using a 100× optical microscope (Leica, DM750, Wetzlar, Germany) to observe cell morphology. Additionally, physiological and biochemical testing were conducted in accordance with the Bergey Bacteriological Testing Manual to further characterize the strain [13] (Table S2).

The primers L11R (5'-TACGACTTAACCCCAATCGC-3') and L11F (5'-AGAGTTT-GATCCTGGCTCAG-3') were specifically designed for the Polymerase Chain Reaction (PCR) molecular biology identification of the L11 strain in the experiment [14]. The PCR amplification conditions employed in the experiment were as follows: an initial denaturation step at 94 °C for 5 min, followed by 30 cycles of denaturation at 94 °C for 1 min, annealing at 56 °C for 20 s, and extension at 72 °C for 60 s. Finally, a terminal extension step was performed at 72 °C for 10 min to ensure the complete amplification of the target DNA fragment. Utilizing these conditions, the 16S rDNA gene sequence of the L11 strain was successfully amplified via PCR. Subsequently, the obtained sequence was compared with the sequence available in the National Center for Biotechnology Information (NCBI) database [15].

2.3. Determination of L11 Reducing Na₂SeO₃ Activity and Culture Conditions

To assess the tolerance of the L11 strain to selenite, the strain was inoculated into fresh LB medium supplemented with varying concentrations of Na₂SeO₃: 0 mM, 2 mM, 5 mM, 10 mM, and 15 mM (1% *v/v*). The light absorption value of the culture was monitored at 600 nm using a microbial growth analyzer (Bioscreen CMBR, Turku, Finland). The plates were incubated at 37 °C for 72 h with continuous shaking at 200 rpm, and absorbance measurements were taken hourly [16].

To further analyze the combined influence of three factors on the biosynthesis of SeNPs in L11, a three-factor and three-level response surface analysis was established in the experiment, and seventeen sets of experiments were designed. Three independent variables were considered: temperature, pH, and rotational speed. The response value was defined as the reduction rate of Na₂SeO₃. The experimental data were analyzed using Design Expert version 12 software (Stat-Ease, Jinshan District, Shanghai, China). Box–Behnken single-factor data and quadratic regression equation were employed for this analysis. ANOVA analysis was performed to assess the significance of the data, with a *p*-value < 0.01 indicating highly significant differences and 0.01 < *p* < 0.05 indicating significant differences. The ideal cultivation conditions were determined by examining the interaction of various factors on the reduction rate of Na₂SeO₃.

2.4. Preliminary Cell Localization of SeNPs

The L11 strain was cultured in an LB-containing triangular flask until it reached the exponential growth phase. The bacterial cells were then centrifuged for 10 min at 4 °C and 12,000× *g* to collect the cell culture. The cell pellet was washed twice with 0.9% NaCl and resuspended before protein extraction. Finally, the corresponding periplasmic, cytoplasmic, membrane, and cell wall components were extracted using the method described by Lampis et al. [17].

2.5. Preparation of SeNPs

The L11 strain was inoculated into a triangular flask containing LB liquid medium supplemented with 4.0 mM Na₂SeO₃. The flask was incubated at 37 °C under agitation at 180 rpm for 12 h to facilitate the biosynthesis of SeNPs. Following incubation, the culture was centrifuged at 12,000× *g* for 10 min to separate the cellular sediment. The precipitate was subsequently washed twice with 0.9% NaCl to remove residual media components and resuspended in 20 mL of Tris-Cl buffer (50 mM, pH 8.2) to stabilize the SeNPs. Subsequently, the sample underwent ultrasonication to disperse the SeNPs, and the resulting suspension was harvested for further analysis, as described by Wang et al. [18].

2.6. Characterization and Analysis of L11 Produced SeNPs

SEM analysis. The L11 strain was inoculated into a triangular flask containing LB liquid medium supplemented with 4 mM Na₂SeO₃. The culture was incubated at 37 °C for 24 h. Subsequently, the bacterial cells were collected by centrifugation and washed three times with 0.9% NaCl solution to remove residual media components. The precipitate was embedded in a precooled fixed solution and fixed overnight at 4 °C. The Hitachi SU 8010 microscope was used for observing strain L11 and the distribution of SeNPs.

TEM analysis. The L11 strain grown for 24 h in LB medium with or without Na₂SeO₃ was subjected to mild centrifugation (5000× g, 5 min) to collect the culture. Mix the precipitate with pre-cooled fixed solution (0.1 M phosphate buffer (PBS), 2% glutaraldehyde, pH 7.4) and fix at 4 °C for 10 min. Subsequently, the L11 strain was centrifuged for 3 min (5000× g). The supernatant was fixed overnight at 4 °C and examined using Hitachi HT-7700 (Tokyo, Japan) TEM at 80.0 KV.

The morphology and chemical elements that constitute SeNPs were identified through SEM-EDS analysis. Before analysis, the SeNPs suspension was dried using a vacuum freeze-drying system (SJIA-10N, Ningbo Yinzhou Sjia Laboratory Equipment Co., Ltd., Yinzhou, China). Then, dry SeNPs were examined using SEM and energy dispersive X-ray spectroscopy (Hitachi S4800, Tokyo, Japan).

The separated SeNPs were analyzed using Zeta Potential (ZP) and size distribution [2]. SeNPs were dispersed in deionized water, sonicated for 10 min, and then approximately 0.5 mL of suspension was transferred to a colorimetric dish impregnated with a cell kit for particle size distribution ZP analysis.

2.7. Sheep Feeding Experiment

The experimental sheep were randomly assigned to a control group and an experimental group, with each group consisting of three parallel replicates. Within each replicate, 10 sheep were selected, ensuring consistency in breed, parity, age, and physical condition. Healthy sheep, regardless of breed, were chosen for this study. The control group was fed a standard diet, whereas the experimental group received a solid bacterial preparation containing SeNPs at a concentration of 80 mg/kg. After 40 days, blood samples were collected to assess serum immune markers and the Se content in various tissues of both groups.

2.8. Determination of Physiological and Biochemical Indicators in Sheep Blood

On the 40th day of the experiment, EDTA-K2 anticoagulant tubes were used to collect jugular vein blood from the experimental group and the control group of sheep, and the cell contents were quickly measured using a fully Automatic Hematology Analyzer (TEK5000P, Jiangxi Tekang Technology Co., Ltd., Nanchang, China). The content of the red blood cells (RBCs), white blood cells (WBCs), and lymphocytes in sheep jugular vein blood was determined according to the method of Alagawan et al. [19].

Part of the blood was centrifuged for 10 min (3000× g), and the supernatant was frozen to −20 °C. The antioxidant indicators of the sheep serum are operated according to the instructions on the IgG, SOD (superoxide dismutase), MDA (malondialdehyde), T-AOC (total antioxidant capacity), and GSH-Px (glutathione peroxidase) detection kit. The above test kits were all purchased from Wuhan Leibelide Technology Co., Ltd. (Wuhan, China), including blood IgG antibody test kits (batch number 201809), SOD kit (batch number 201809), MDA kit (batch number 201809), T-AOC kit (batch number 201809), GSH-Px kit (batch number 201809).

2.9. Statistic Analysis

Excel 2021 v2212 (Microsoft, Raymond, WA, USA) and SPSS v22.0 (IBM, Amonk, NY, USA) were used for the processing and analysis of all data. The data between treatment groups were compared using Duncan's test, with $p < 0.05$ indicating statistical significance. Three biological replicates were measured for each group of processed data. The data analysis results were plotted using Origin 2019 software (Microcal Software,

Northamptonshire, MA, USA). The phylogenetic tree of L11 strain 16S rDNA was constructed by MEGA version 7.0 with a neighbor-joining (NJ) method and measured by bootstrap analysis with 1000 replicates.

3. Results and Discussion

3.1. Isolation and Identification of Strain L11

The individual cell of L11 is rod-shaped, and the two ends of the cell are relatively flat (Figure 1A). The colony of L11 is circular, with irregular edges and a smooth and moist surface. The colony is opaque and slightly grayish white, with a diameter of about 1–2 mm. It is Gram-positive and produces spores, with spores growing in the middle (Figure 1B). Table S2 shows the Biolog GENIII identification of the L11 strain, which was compared with the data in the Biolog strain database. The results showed that, after 16 h of cultivation, the similarity value between L11 and *B. subtilis* was 0.921, and the dissimilarity was 4.246. The likelihood of L11 being identified as *B. subtilis* was 100%.

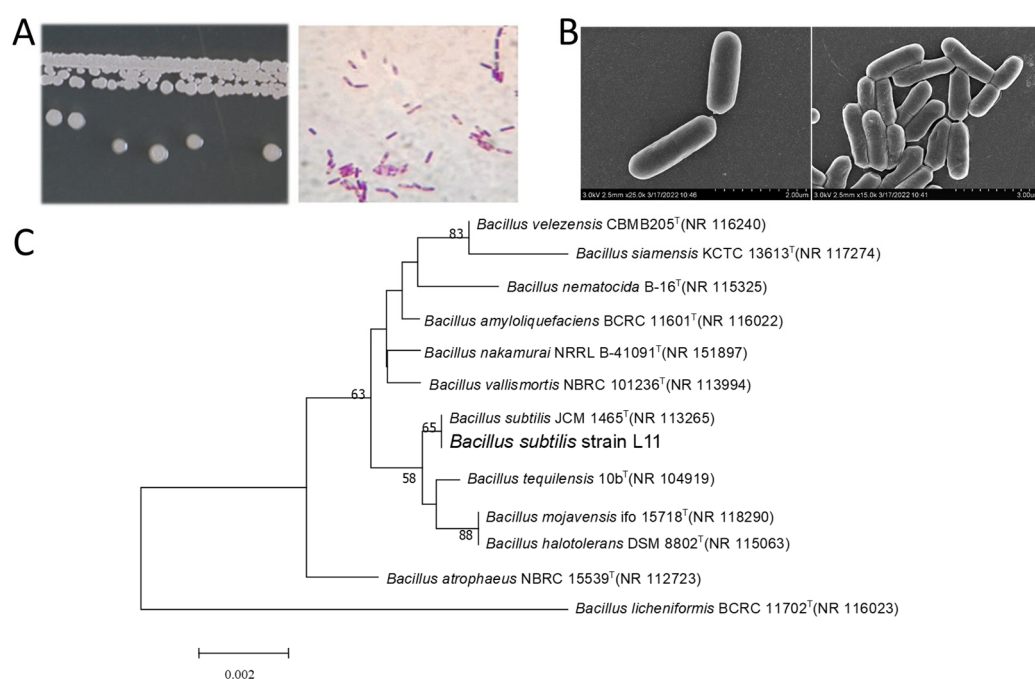


Figure 1. Morphological, physiological, and molecular biological identification of L11 strain. (A) Identification of colony morphology and optical microscopy observation of L11. (B) Scanning electron microscopy observation of L11 colony. (C) Phylogenetic tree analysis of 16s DNA sequences between L11 strain and other related species. The phylogenetic tree was constructed using the neighboring connection method of MEGA 7.0 software and subjected to 1000 repeated similarity calculations. The nodes of the phylogenetic tree in the figure only display values with bootstrap values greater than 50%, and the superscript “T” represents the mode strain. The numerical value of the scale bar was 0.002, which indicated that each unit length of branch in the phylogenetic tree represented a relative genetic distance of 0.002.

Following sequencing, the 16S rDNA of the L11 strain was submitted to the GenBank database for Basic Local Alignment Search Tool (BLAST) analysis. Based on the Blast results, a phylogenetic tree was constructed to further elucidate the taxonomic position and evolutionary relationships of the L11 strain within its bacterial clade. The results showed that the genus *Bacillus* had the highest homology with L11. The 16S rDNA sequence of L11 was compared with several strains with a higher homology in the database, and multiple sequence alignments were performed using ClusterX. The phylogenetic tree reveals L11 clusters within a branch alongside *B. subtilis* JCM1465T, exhibiting 98% homology in its 16S rDNA sequence. This finding reinforces the aforementioned preliminary identification

outcomes. Taking into account the morphological, physiological, and biochemical characteristics of L11, along with the sequence analysis of its 16S rDNA, L11 was confidently identified as *B. subtilis* (Figure 1C).

3.2. Optimization of Growth Conditions for L11 Strain

In the universal culture medium of *Bacillus*, L11 reached its maximum bacterial concentration at 25–26 h, and after 30 h, it showed a slow downward trend. In the LB medium, the growth rate of L11 showed a rapid growth trend from 0 to 40 h, and after 40 h, the growth rate of L11 slowed down. Overall, the growth status of L11 in LB medium is better than that in *Bacillus* universal medium (Figure 2A). Under the conditions of 30–37 °C, the growth concentration of the L11 strain showed an upward trend. Among them, L11 has the best growth state at 37 °C (Figure 2B). At 37 °C, 120 rpm, and in LB media, the growth concentration of L11 was maintained within a stable range when the pH value was between 5 and 9, and the growth status of L11 was ideal at pH = 6 (Figure 2C). Under the ideal cultivation conditions mentioned above, the faster the shaking culture speed, the higher growth concentration of the L11 strain. When the shaking speed was 200 rpm, the concentration of L11 solution reaches its maximum (Figure 2D). Therefore, the ideal growth conditions for the L11 strain can be set as LB medium, oscillating culture at 37 °C, pH = 6, and 200 rpm.

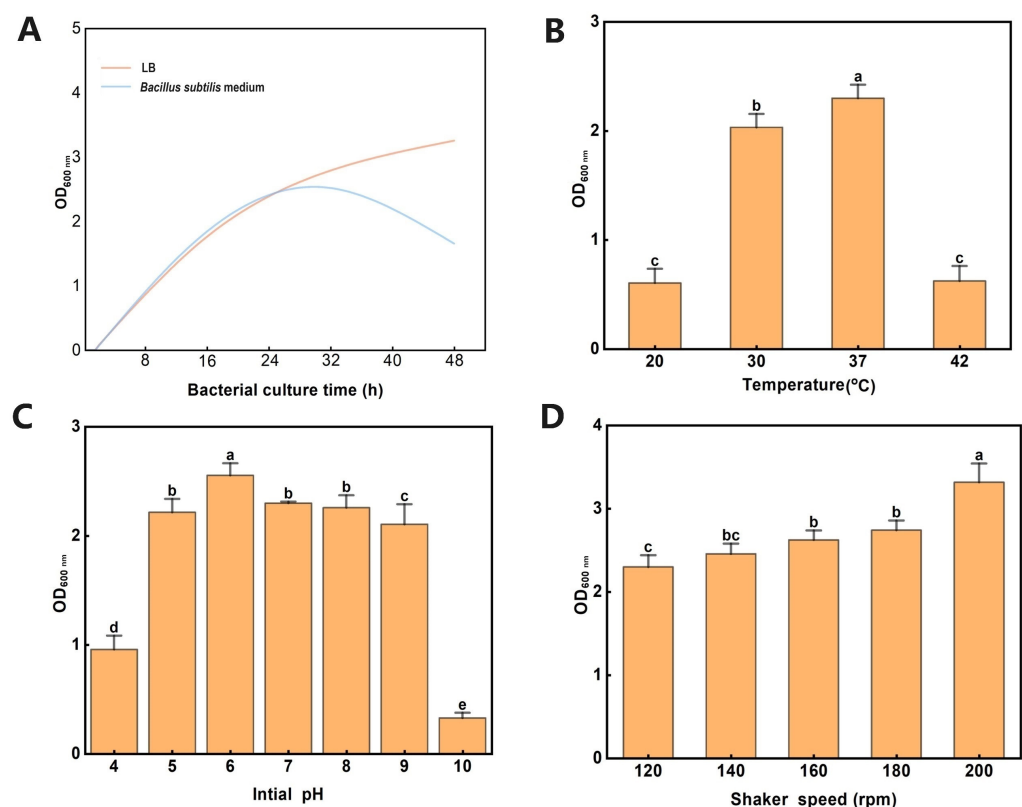


Figure 2. The growth rate of L11 strain under different culture conditions, and the vertical axis OD_{600nm} represents the absorbance value of the bacterial solution at a wavelength of 600 nm. The error bar represents the standard error of the mean ($n = 3$), and different letters represent the different level between the mean values of Duncan's new complex range test ($p < 0.05$). (A) The growth status of L11 in two different media. (B) The effect of temperature on the growth of *B. subtilis* L11. (C) The effect of pH value on the growth of L11 strain. (D) The effect of cultivation speed on the growth of L11 strain.

3.3. Optimization of Synthesis Conditions for SeNPs by L11

In order to determine the Na₂SeO₃ concentration and maximum reduction rate that L11 strain can tolerate, different concentrations of Na₂SeO₃ cultivation conditions were

designed under the ideal growth conditions of L11. The results showed that, when the final concentration of Na_2SeO_3 was 5–15 mmol/L, the Se content and Se reduction rate in the culture medium rapidly decreased with the increase in concentration. When the concentration was 10 and 15 mmol/L, strain L11 hardly produces SeNPs, and the growth of L11 is also inhibited. This indicated that the ideal cultivation concentration of Na_2SeO_3 lies outside the range of 5–15 mmol/L (Table S3). When the concentration of Na_2SeO_3 was 4 mmol/L and the cultivation time was 48 h, the Se reduction rate of strain L11 reached 72%. When the cultivation time was 72 h, the reduction rate reached 73.5%. This indicates that only 1.5% of Na_2SeO_3 was reduced within 48–72 h, so the ideal cultivation time was selected as 48 h (Table S4). Previous studies have demonstrated that the absence of a decrease in selenite levels during the stationary phase of bacterial growth indicates that the reduction in Se(IV) primarily occurs during the initial growth phase of the bacteria [12]. When the Se concentration in the culture medium is high, the detoxification process of microorganisms is activated, producing reduced Se^0 . By changing the color, it is possible to preliminarily determine the reduced Se produced by microorganisms. When amorphous Se^0 is formed, the cell color is red. When the crystalline Se^0 forms, the cell color turns gray, indicating that toxic and colorless selenite has been converted into non-toxic SeNPs [20].

The cultivation at different temperatures affects the efficiency of L11 in converting SeNPs (Figure 3A). Within the temperature range of 20–37 °C, the production of SeNPs by strain L11 exhibits a positive correlation with increasing temperature. However, as the temperature rises from 37 °C to 42 °C, the conversion rate of SeNPs begins to decline. Therefore, the most suitable temperature for strain L11 to convert SeNPs is 30–37 °C, which is consistent with the ideal temperature for L11 growth. The concentration of strain L11 at 42 °C was higher than that at 20 °C, indicating that the addition of Na_2SeO_3 to the culture medium improved the strain's high-temperature resistance to a certain extent, but the production of SeNPs decreased. When the cultivation temperature is significantly higher than the ideal growth temperature, bacterial growth is inhibited. When the cultivation temperature is lower than the ideal growth temperature of bacteria, their metabolic activity is inhibited [21].

As the oscillation speed of the culture medium increases, the conversion rate of SeNPs shows a trend of first increasing and then decreasing. When the rotational speed is 100 rpm, the conversion rate of SeNPs reaches its maximum value, and then the conversion rate begins to decrease as the rotational speed increases (Figure 3B). Therefore, a culture medium speed of 100 rpm is more conducive to the reduction of selenite by L11 strain.

The results in Figure 3C indicate that, as the initial pH value of the culture medium increases, the conversion rate of the strain L11 reducing selenite shows a trend of first increasing and then decreasing. When the initial pH of the culture medium is 6.0, the conversion rate reaches its maximum value, which may be related to the ideal growth pH of L11 being 6.0.

The response surface analysis of L11 strain's reduction of Na_2SeO_3 revealed that the strain exhibited the highest reduction rate of Na_2SeO_3 when the pH of the culture medium was 6, the temperature was 37 °C, and the agitation speed was 150 rpm (Figure 3D). In the *Bacillus* sp. BSN313 strain, the optimal conditions for the reduction and production of SeNPs occur at a temperature of 37 °C and a higher rotation speed of 200 rpm [2]. Similar cultivation conditions have been observed in *B. subtilis* 168 strain, with a pH of 7, which was slightly higher than the pH used in the present study [12]. This variation may be attributed to the optimal pH for reduction varying among different bacterial strains. However, in the context of optimizing growth conditions for strain L11 in this study, while 37 °C and 200 rpm were identified as ideal, it was observed that a reduction in rotation speed was necessary to achieve the highest reduction rate during SeNP production.

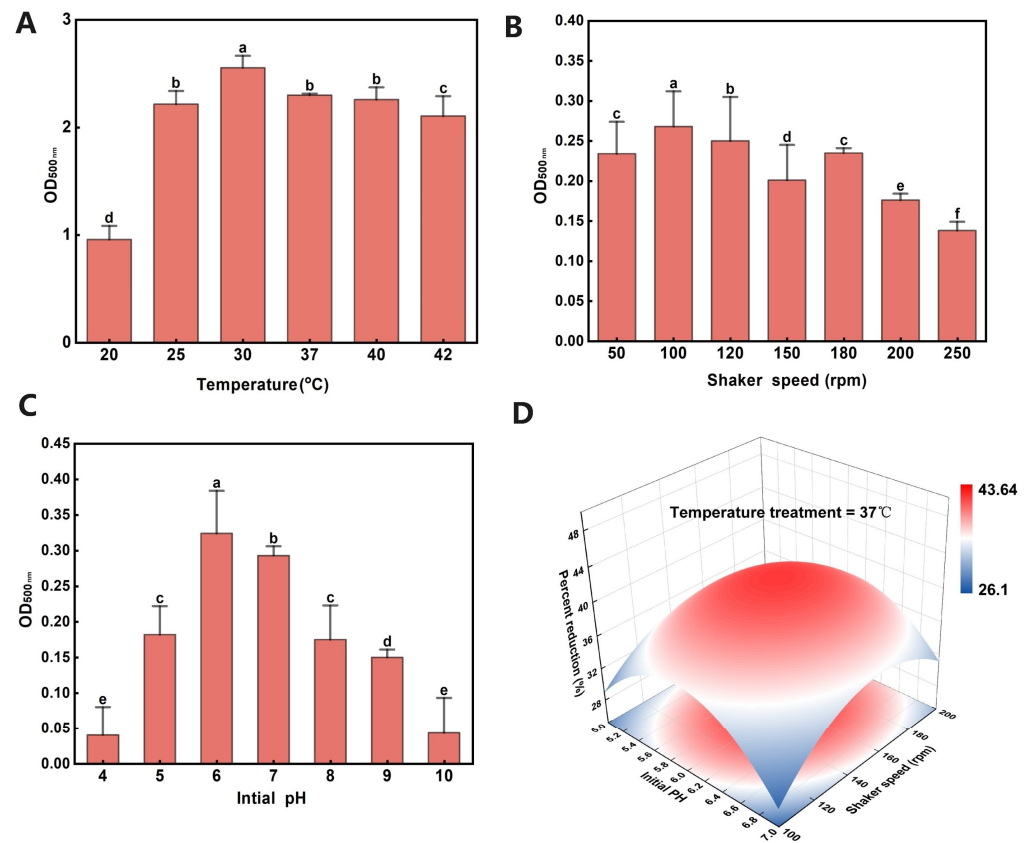


Figure 3. Optimization of conditions for L11 reduction in Na_2SeO_3 to SeNPs. The vertical coordinate labeled $\text{OD}_{500\text{nm}}$ in the figure denotes the precise wavelength at which the maximum absorption peak of L11 occurs during the production of SeNPs, specifically at 500 nm. The error bar represents the standard error of the mean ($n = 3$), and different letters represent the difference level between the mean values of Duncan's new complex range test ($p < 0.05$). **(A)** The effect of cultivation temperature on the production of SeNPs by strain L11. **(B)** The effect of cultivation speed on the production of SeNPs by L11. **(C)** The effect of pH value of culture medium on the production of SeNPs by L11. **(D)** Response surface analysis of the effects of temperature, rotational speed, and pH on the production of SeNPs by L11 strain.

3.4. L11 Subcellular Localization Analysis of SeNPs

To analyze the localization of SeNPs produced by L11 strain in cells, proteins from the different parts of L11 cells were isolated and their content in different protein components was displayed. As shown in Figure 4, with the addition of Na_2SeO_3 in the culture medium, the periplasmic space proteins of L11 cells showed a light red color, while the crude extract of cell membrane and cell wall proteins showed a red color, while the control group showed colorless secretion proteins, cell membrane, and cell wall proteins. The results indicate that the reduction of Na_2SeO_3 by *B. subtilis* L11 to produce red SeNPs mainly occurs in the periplasmic space, cell membrane, and cell wall. Microorganisms will utilize high-valence Se (Se^{4+} or Se^{6+}) in the environment as electron acceptors to convert it into SeNPs. Some microorganisms convert high-valence Se into elemental Se particles outside the cell, while others convert sodium selenate or Na_2SeO_3 into elemental SeNPs within the cell, and then use special mechanisms to expel intracellular SeNPs out of the cell [22].

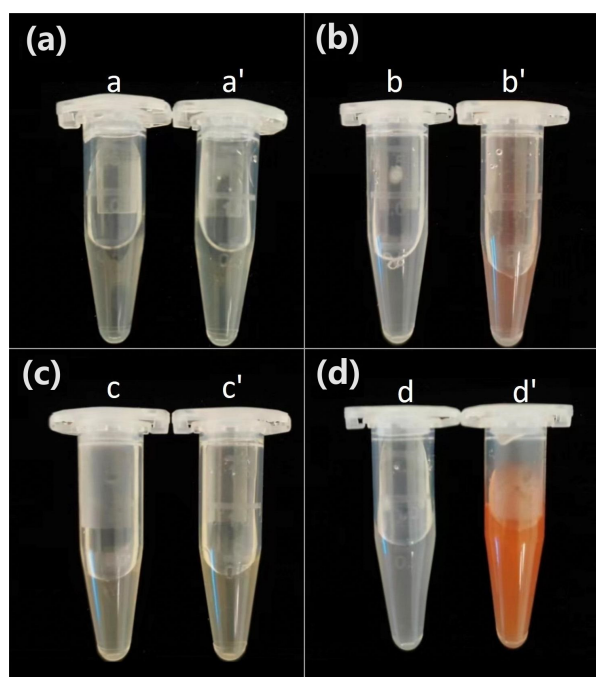


Figure 4. Subcellular localization of SeNPs transformed by *B. subtilis* L11. (a) Extracellular secreted proteins in L11 culture (a—exocrine proteins without Na_2SeO_3 added to the culture medium; a'—the exocrine protein of Na_2SeO_3 was added to the culture medium). (b) Periplasmic space proteins of L11 culture (b—periplasmic space proteins of L11 cells without Na_2SeO_3 added to the culture medium; b'—periplasmic space proteins with Na_2SeO_3 added to the culture medium). (c) Cytoplasmic protein extract of L11 culture (c—cytoplasmic proteins without Na_2SeO_3 added to the culture; c'—cytoplasmic protein with added Na_2SeO_3). (d) Extracts of cell membrane and cell wall proteins from L11 culture (d—cell membrane and cell wall proteins without Na_2SeO_3 added to the culture medium. d'—cell membrane and cell wall proteins with added Na_2SeO_3).

3.5. Analysis of SEM and EDS Spectra of L11 Strain Producing SeNPs

Strain L11 was inoculated into LB medium, both with and without the addition of Na_2SeO_3 , for cultivation purposes. Following a 48 h incubation period, the precipitates were collected by centrifugation to obtain the culture. Subsequently, the culture was immobilized and subjected to SEM and EDS analysis for a detailed observation and elemental characterization. The biosynthesis results of SeNPs are shown in Figure 5. Figure 5a–f showed the SEM observation results and EDS test results of the culture without adding Na_2SeO_3 , while Figure 5g–l showed the corresponding experimental group test results. Comparing the SEM images of cultures depicted in Figure 5a,g, it was evident that a significant amount of spherical particulate matter was clustered around the L11 cells of the experimental group. In contrast, the control group cells exhibited no particulate matter surrounding them.

The EDS analysis of the elemental composition in Figure 5a,g demonstrated the presence of Se in the experimental group culture, whereas the control group lacked this element. The specific mass fraction and atomic number fraction of certain elements in the analyzed region were detailed in Table 1. Notably, the mass fraction and atomic number fraction of Se in the control group were both 0, indicating its absence. In contrast, the experimental group exhibited a mass fraction of 0.47% and an atomic number fraction of 0.07% for Se. The elemental distribution analysis, as presented in Figure 5c–f,i–l, provided further evidence that Se was exclusively present in the experimental group. This was corroborated by the SEM observations in Figure 5g, which were found to be in agreement with the EDS results (Figure 5l) regarding the distribution of Se. Collectively, these findings confirm the presence of Se within the particles aggregated around the cells, with a particle

size ranging from 50 to 200 nm. Some studies have shown that the size of SeNPs plays a major role in their biological activity. Usually, smaller particles are more effective than larger particles [23,24]. Smaller SeNPs increase their biological activity by enhancing the action of thioredoxin reductase and selenidase peroxidase [25]. In addition, the toxicity of smaller SeNPs is much lower than that of larger ones [26].

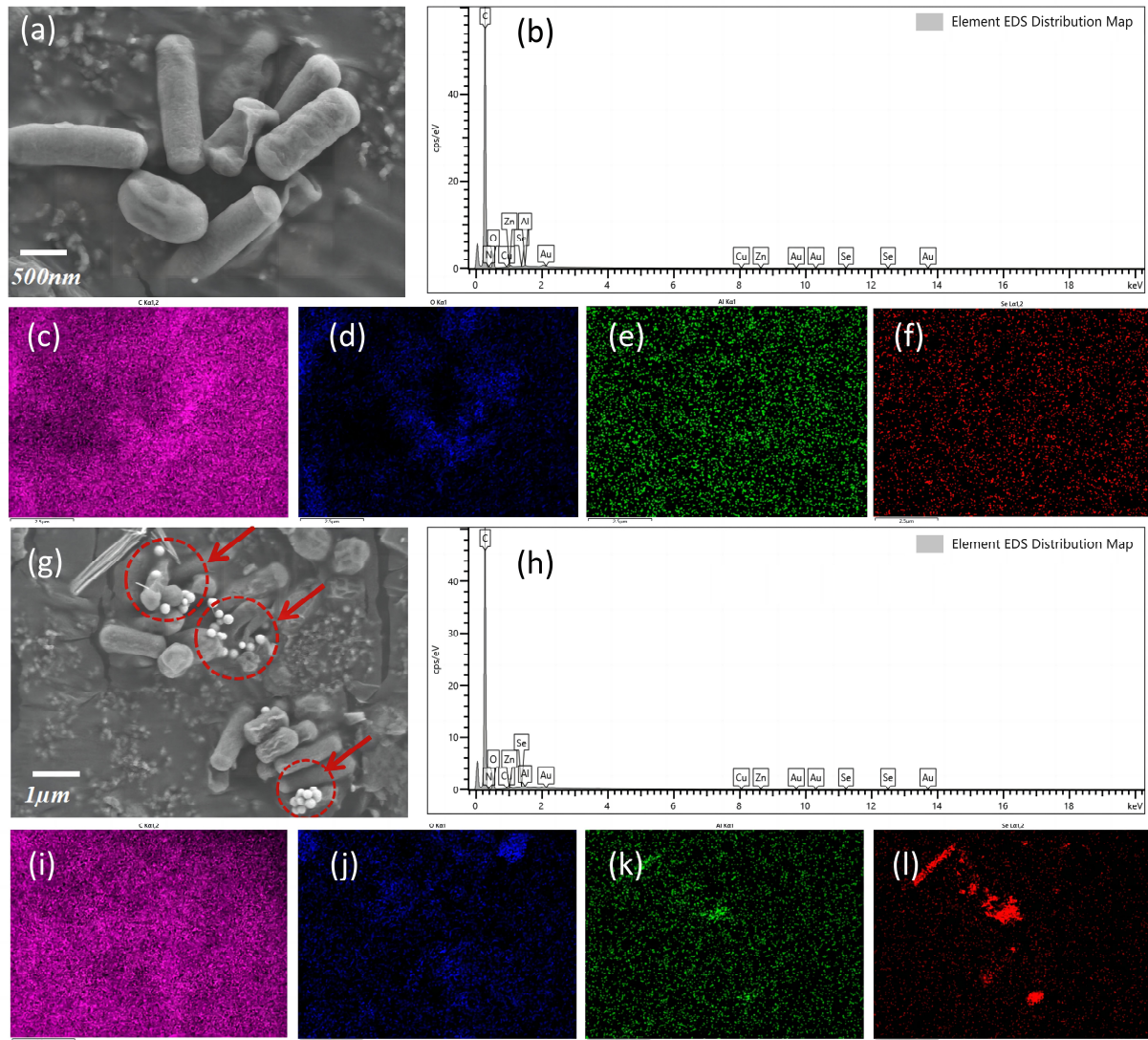


Figure 5. Scanning Electron Microscope-Energy Dispersive Spectroscopy (SEM) and Energy Dispersive Spectroscopy (EDS) spectra analysis of Selenium nanoparticles (SeNPs) as a reducing product of L11. (a) SEM image of culture without added Na_2SeO_3 . (b) EDS diagram of some elements in culture without adding Na_2SeO_3 . (c) Distribution of carbon elements in the control group. (d) Distribution of oxygen elements in the control group. (e) Distribution of aluminum elements in the control group. (f) Se distribution in the control group. (g) The SEM image of the culture supplemented with Na_2SeO_3 reveals the presence of SeNPs secreted by strain L11. The dashed circles and arrows in the image indicate the SeNPs produced by the L11 cells. (h) EDS diagram of some elements in the culture with added Na_2SeO_3 . (i) Carbon element distribution in the experimental group. (j) Distribution of oxygen elements in the experimental group. (k) Distribution of aluminum elements in the experimental group. (l) Distribution of Se elements in the experimental group.

Table 1. Mass fraction and atomic number fraction of some elements in the growth area of strain L11.

Element	Control		Experimental Group	
	Element Mass Fraction	Atomic Fraction	Element Mass Fraction	Atomic Fraction
C	79.55	83.15	83.26	86.70
N	7.95	7.13	5.71	5.10
O	12.29	9.64	10.23	8.00
Al	0.14	0.06	0.24	0.11
Cu	0.04	0.01	0.03	0.01
Zn	0.03	0.01	0.06	0.01
Se	0.00	0.00	0.47	0.07
Au	0.00	0.00	0.00	0.00

3.6. XPS Analysis of SeNPs as a Reduction Product of L11

In order to accurately verify the valence state of Se obtained by the L11 reduction of Na_2SeO_3 , XPS Peak software V4.1 (Thermo Fisher Scientific, Waltham, MA, USA) was used to fit the Se 3D peak. The results showed that the peak of Se 3d5 was at 55.49 eV, while the peak of Se 3d3 was at 56.24 eV (Figure 6). According to the report by Han et al. [27], the Se 3D peak binding energy of Se(IV) was greater than 58.0 eV, with the elemental Se ranging from 54.6 to 57.5 eV, and Se compounds ranging from 52.8 to 55.7 eV. In the present study, the binding energies of Se 3d5 and Se 3d3 were between 54.6 and 57.5 eV, as reported by Han [27], indicating that the particulate matter in this study was elemental Se. Based on the above EDS analysis results, the particulate matter gathered around L11 cells is biological SeNPs, which is reduced by *B. subtilis* L11 to elemental Se.

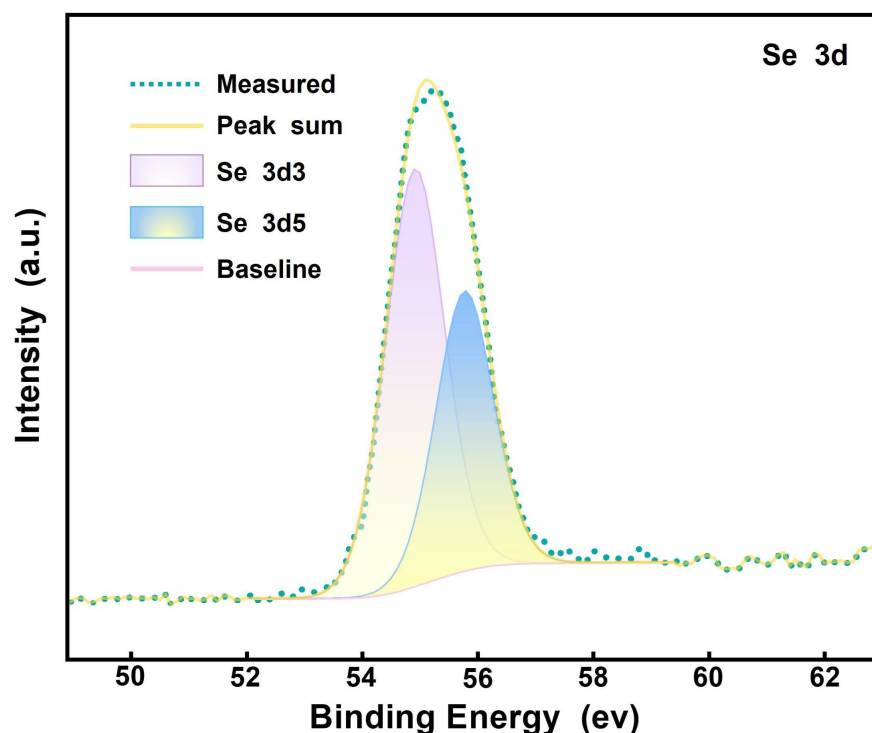


Figure 6. The XPS Peak software was utilized to fit the maximum energy absorption peaks of the reduced products of Na_2SeO_3 transformed by strain L11 in the Se 3d5 and Se 3d3 regions. The energy absorption peak of Se 3d5 is 55.1 eV, while the energy absorption peak of Se 3d3 is 56 At eV.

3.7. TEM Characterization and Particle Size Analysis of SeNPs Produced by L11

The TEM observation results indicate that L11 produces the spherical nanoparticles of Se (Figure 7), with particle sizes mainly distributed between 100 and 200 nm. In the

ultra-thin sections of *B. subtilis* L11 cultured without adding Na_2SeO_3 , no significant SeNPs particles were observed both intracellular and extracellular (Figure 7a,c). In the ultra-thin section of L11 culture with Na_2SeO_3 added, both intracellular and extracellular SeNPs are present (Figure 7b,d), and extracellular SeNPs are also expelled from the field of view (Figure 7b,e). In the cell localization experiment of L11 transformation to produce the SeNPs mentioned above, it was found that red substances were present in both the periplasmic space proteins and the rough extract of the cell membrane cytoplasm (Figure 4). Electron microscopy analysis of the reduced product confirmed that this product was SeNPs, which indicates that L11 produces SeNPs synthesized within L11 cells and then released into the extracellular space (Figure 7d,e). The size of SeNPs produced by L11 was slightly smaller than that in *B. niabensis* [28], and the shape of the SeNPs obtained by reducing selenite by the *A. brasilense* strain is basically the same [29]. The smaller the size of SeNPs, the higher its inhibitory effect on *E. coli*, *P. aeruginosa*, and *S. aureus* [1].

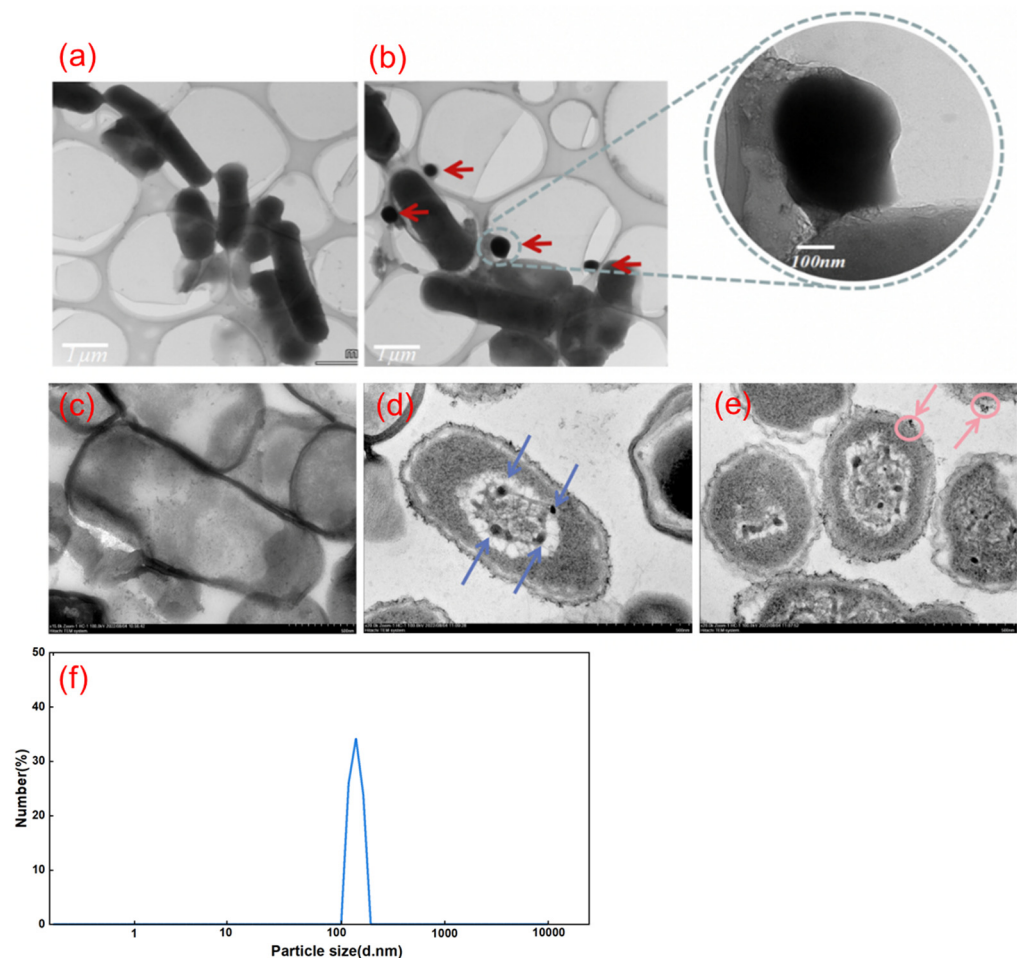


Figure 7. Transmission Electron Microscopy (TEM) characterization analysis of L11 reduction product SeNPs. (a) TEM characterization of culture without Na_2SeO_3 addition. (b) TEM characterization of SeNPs as a reduction product of Na_2SeO_3 . The red arrow indicated the extracellularly secreted selenium nanoparticles. (c) Culture bacteria without added Na_2SeO_3 . (d) SeNPs distributed within the cell of L11. The blue arrow indicated the intracellularly synthesized selenium nanoparticles. (e) Simultaneous distribution of SeNPs in both the intracellular and extracellular regions of L11. The pink arrow indicates the SeNPs that were being secreted from the intracellular space to the extracellular environment. (f) Particle size analysis of the reduction product SeNPs produced by L11.

Some bacteria rely on the non-specific selenite reductase system in the periplasmic space to reduce selenite to elemental Se. The red SeNPs generated during the reduction process accumulates in the cytoplasm and extracellular space to form SeNPs [22]. The

preliminary cell localization and TEM images of L11 transformation to produce SeNPs can confirm that the reduction of Na_2SeO_3 by L11 strain to generate SeNPs is synthesized within the cytoplasm and transported to the extracellular space. This is consistent with the synthesis of SeNPs by *Ochrobactrum* sp. MPV1, but different from the way that *Thauera selenati* synthesizes SeNPs in the cytoplasm and transports it out of the cell [22,30,31].

3.8. Preliminary Study on the Application of L11 to Produce SeNPs

In order to preliminarily analyze the application of the L11 strain in livestock and poultry, this study added SeNPs-rich L11 solid bacterial agent to the conventional feed of sheep, and fed it according to the conventional feeding method of sheep. The experimental results showed that the IgG, T-AOC, GSH-Px, and SOD contents of the experimental group were significantly higher than those of the control group ($p < 0.01$), while the white blood cell and lymphocyte and MDA (malondialdehyde) contents were significantly lower ($p < 0.01$) than those of the control group, whilst the difference in the red blood cell content was not significant ($p > 0.05$) (Table 2). The experimental results indicated that adding SeNPs rich L11 bacterial agent to feed can significantly improve the immunity of sheep. Compared with the control group, broilers supplemented with Se-rich *B. subtilis* not only gained weight, but also increased enzyme activities such as the GPx, CAT, POD, and plasma levels of IL-2, IL-4, and IgG, while plasma MDA levels decreased [32]. After oral administration, some *B. subtilis* strains can colonize the intestinal mucosa of animals, optimize the composition of intestinal microbiota, and effectively stimulate immunity and metabolism. These can enhance the animal's resistance to intestinal diseases, stress, and the clearance of pathogens [33]. Supplementing a certain amount of Se can regulate the gastrointestinal metabolism and antioxidant performance. In addition, Se can enhance the immune cell defense against pathogens that cause infection [34]. In addition, supplementing Se can regulate the bacterial composition in the gastrointestinal tract, thereby promoting physical health [35,36]. Yang et al. prepared an Se-rich *B. subtilis* strain and added it to the diet of broilers. By colonizing and regulating the gut microbiota population, the production performance and immunity of broilers were improved [37].

Table 2. The effect of L11-rich SeNPs bacterial agent on sheep immunity.

Test Items	Control	Experimental Group
RBC ($10^{12}/\text{L}$)	5.53 ± 0.12	5.61 ± 0.12
WBC ($10^9/\text{L}$)	152.34 ± 39.46	$9.56 \pm 4.11^{**}$
Lymphocyte count ($10^9/\text{L}$)	137.51 ± 32.73	$7.38 \pm 0.89^{**}$
IgG ($\mu\text{g}/\text{mL}$)	896.46 ± 79.66	$1637.13 \pm 39.75^{**}$
SOD (U/mL)	268.97 ± 24.24	$392.28 \pm 10.19^{**}$
MDA (nmol/mL)	172.54 ± 11.08	$149.59 \pm 12.33^{**}$
T-AOC (U/mL)	47.46 ± 1.98	$56.22 \pm 1.91^{**}$
GSH-Px (U/mL)	784.25 ± 28.37	$1163.74 \pm 18.68^{**}$

Note: ** indicates extremely significant differences ($p < 0.01$), and the results are expressed as mean \pm standard error.

The results in Table 3 indicate that the Se content in the neck muscles, liver, and spleen tissues of sheep in the experimental group supplemented with L11 Se-rich nanobacteria in the feed was significantly higher than that in the control group ($0.01 < p < 0.05$), and the Se content in the lungs did not reach a significant level ($p > 0.05$). Therefore, adding SeNPs-rich L11 bacterial agent to feed can increase the total Se content in livestock muscles and viscera. In Tibetan sheep, after being fed with Se-containing lactic acid bacteria, the total Se content in neck muscle, liver, and spleen was significantly higher than that of the control group, while the Se content in the lungs was the same as that of the control group. This indicates that the liver, muscle, and spleen are the main tissues and organs for Se accumulation in sheep, which is consistent with the results of this study [38].

Table 3. The effect of feeding L11-enriched SeNPs bacteria on Se content in sheep tissues.

Test Items	Control	Experimental Group
Neck muscles (mg/kg)	0.07 ± 0.02	0.13 ± 0.001 *
Liver (mg/kg)	0.36 ± 0.05	0.96 ± 0.13 *
Lungs (mg/kg)	0.29 ± 0.04	0.41 ± 0.05
Spleen (mg/kg)	0.31 ± 0.03	0.62 ± 0.07 **

Note: * indicates significant differences ($0.01 < p < 0.05$), ** indicates extremely significant differences ($p < 0.01$), and the results are expressed as mean ± standard error.

4. Conclusions

In this study, a *Bacillus subtilis* strain designated as L11, capable of producing SeNPs, was isolated and screened. The optimal cultivation conditions and Na_2SeO_3 concentration for SeNP production by strain L11 were subsequently determined through rigorous optimization procedures. Subcellular compartment analysis revealed that L11 primarily generates SeNPs within the periplasmic space, cell membrane, and cell wall of the transformed cells. Furthermore, the detailed characterization of the produced SeNPs was performed using XPS, SEM-EDS, and TEM, confirming the presence of nanoparticles with a diameter ranging from 50 to 200 nm. The chemical properties and composition of the particle surfaces were also determined. When the L11–SeNPs complex was added to sheep feed, it significantly enhanced the sheep’s antioxidant enzyme activity and immune response, leading to an increase in Se content in the neck muscle, liver, and spleen tissues of the sheep.

Supplementary Materials: The following supporting information can be downloaded at: <https://www.mdpi.com/article/10.3390/microbiolres15010022/s1>, Table S1: Quantification of the growth of strain L11 in two different media; Table S2: The identification results of endophytic bacteria L11; Table S3: The first step screening of Na_2SeO_3 culture concentration for L11 strain; Table S4: The second step screening of Na_2SeO_3 culture concentration for the L11 strain.

Author Contributions: Investigation, Formal analysis, Methodology, Software, Data curation, W.G.; Software, Formal analysis, Visualization, X.S.; Methodology, Software, Formal analysis, L.W.; Funding acquisition, Investigation, X.C.; Validation, Investigation, S.C.; Experiment, Resources, Investigation, Writing—review and editing, L.L.; Conceptualization, Resources, Writing—original draft, Supervision, H.C. All authors have read and agreed to the published version of the manuscript.

Funding: The research was funded by the Horizontal science and technology of Enshi Se-De Bioengineering Co., Ltd., grant number se1-202102.

Institutional Review Board Statement: The work related to animal testing in this study has been approved by the Ethics Committee of the School of Modern Industry for Selenium Science and Engineering, Wuhan Light Industry University. The approval code was WHSE20230021.

Informed Consent Statement: Not applicable.

Data Availability Statement: The data used to support the findings of this study can be made available by the corresponding author upon request.

Conflicts of Interest: The authors declare no conflicts of interest.

References

- Nikam, P.B.; Salunkhe, J.D.; Minkina, T.; Rajput, V.D.; Kim, B.S.; Patil, S.V. A review on green synthesis and recent applications of red nano selenium. *Results Chem.* **2022**, *4*, 100581. [[CrossRef](#)]
- Ullah, A.; Yin, X.; Wang, F.; Xu, B.; Mirani, Z.A.; Xu, B.; Chan, M.W.; Ali, A.; Usman, M.; Ali, N.; et al. Biosynthesis of selenium nanoparticles (via *Bacillus subtilis* BSN313), and their isolation, characterization, and bioactivities. *Molecules* **2021**, *26*, 5559. [[CrossRef](#)]
- Nayak, V.; Singh, K.R.B.; Singh, A.K.; Singh, R.P. Potentialities of selenium nanoparticles in biomedical science. *New J. Chem.* **2021**, *45*, 2849–2878. [[CrossRef](#)]
- Yang, J.; Wang, J.; Yang, K.; Liu, M.; Qi, Y.; Zhang, T.; Fan, M.; Wei, X. Antibacterial activity of selenium-enriched lactic acid bacteria against common food-borne pathogens in vitro. *J. Dairy Sci.* **2018**, *101*, 1930–1942. [[CrossRef](#)] [[PubMed](#)]

5. Quinn, C.F.; El Mehdawi, A.F.; Pilon-Smits, E.A.H. Ecology of Selenium in Plants. In *Selenium in Plants: Molecular, Physiological, Ecological and Evolutionary Aspects*; Pilon-Smits, E.A.H., Winkel, L.H.E., Lin, Z.-Q., Eds.; Springer International Publishing: Cham, Switzerland, 2017; pp. 177–188.
6. Gupta, M.; Gupta, S. An overview of selenium uptake, metabolism, and toxicity in plants. *Front. Plant Sci.* **2017**, *7*, 2074. [[CrossRef](#)] [[PubMed](#)]
7. Bajaj, M.; Schmidt, S.; Winter, J. Formation of Se (0) nanoparticles by *Duganella* sp. and *Agrobacterium* sp. isolated from Se-laden soil of North-East Punjab, India. *Microb. Cell Factories* **2012**, *11*, 64. [[CrossRef](#)] [[PubMed](#)]
8. Shoeibi, S.; Mozdziak, P.; Golkar-Narenji, A. Biogenesis of selenium nanoparticles using green chemistry. *Top. Curr. Chem.* **2017**, *375*, 88. [[CrossRef](#)] [[PubMed](#)]
9. Khoei, N.S.; Lampis, S.; Zonaro, E.; Yrjälä, K.; Bernardi, P.; Vallini, G. Insights into selenite reduction and biogenesis of elemental selenium nanoparticles by two environmental isolates of *Burkholderia fungorum*. *New Biotechnol.* **2017**, *34*, 1–11. [[CrossRef](#)] [[PubMed](#)]
10. Ikram, M.; Javed, B.; Raja, N.I.; Mashwani, Z.R. Biomedical potential of plant-based selenium nanoparticles: A comprehensive review on therapeutic and mechanistic aspects. *Int. J. Nanomed.* **2021**, *2021*, 249–268. [[CrossRef](#)] [[PubMed](#)]
11. Ali, F.; Saeed, K.; Fatemeh, H. Nano-bio selenium synthesized by *Bacillus subtilis* modulates broiler performance, intestinal morphology and microbiota, and expression of tight junction's proteins. *Biol. Trace Elem. Res.* **2022**, *200*, 1811–1825. [[CrossRef](#)] [[PubMed](#)]
12. Jia, H.; Huang, S.; Cheng, S.; Zhang, X.; Chen, X.; Zhang, Y.; Wang, J.; Wu, L. Novel mechanisms of selenite reduction in *Bacillus subtilis* 168: Confirmation of multiple-pathway mediated remediation based on transcriptome analysis. *J. Hazard. Mater.* **2022**, *433*, 128834. [[CrossRef](#)] [[PubMed](#)]
13. Bergey, D.H. *Bergey's Manual of Determinative Bacteriology*, 9th ed.; Lippincott Williams & Wilkins: Baltimore, MD, USA, 1994.
14. Janda, J.M.; Abbott, S.L. 16S rRNA gene sequencing for bacterial identification in the diagnostic laboratory: Pluses, perils, and pitfalls. *J. Clin. Microbiol.* **2007**, *45*, 2761–2764. [[CrossRef](#)] [[PubMed](#)]
15. Yoon, S.-H.; Ha, S.-M.; Kwon, S.; Lim, J.; Kim, Y.; Seo, H.; Chun, J. Introducing EzBioCloud: A taxonomically united database of 16S rRNA gene sequences and whole-genome assemblies. *Int. J. Syst. Evol. Microbiol.* **2017**, *67*, 1613. [[CrossRef](#)] [[PubMed](#)]
16. Avendaño, R.; Chaves, N.; Fuentes, P.; Sánchez, E.; Jiménez, J.L.; Chavarría, M. Production of selenium nanoparticles in *Pseudomonas putida* KT2440. *Sci. Rep.* **2016**, *6*, 37155. [[CrossRef](#)] [[PubMed](#)]
17. Lampis, S.; Zonaro, E.; Bertolini, C.; Cecconi, D.; Monti, F.; Micaroni, M.; Turner, R.J.; Butler, C.S.; Vallini, G. Selenite biotransformation and detoxification by *Stenotrophomonas maltophilia* SeITE02: Novel clues on the route to bacterial biogenesis of selenium nanoparticles. *J. Hazard. Mater.* **2017**, *324*, 3–14. [[CrossRef](#)]
18. Wang, Y.; Shu, X.; Zhou, Q.; Fan, T.; Wang, T.; Chen, X.; Li, M.; Ma, Y.; Ni, J.; Hou, J. Selenite reduction and the biogenesis of selenium nanoparticles by *Alcaligenes faecalis* Se03 isolated from the gut of *Monochamus alternatus* (Coleoptera: Cerambycidae). *Int. J. Mol. Sci.* **2018**, *19*, 2799. [[CrossRef](#)]
19. Alagawany, M.; Madkour, M.; El-Saadony, M.T.; Reda, F.M. *Paenibacillus polymyxa* (LM31) as a new feed additive: Antioxidant and antimicrobial activity and its effects on growth, blood biochemistry, and intestinal bacterial populations of growing Japanese quail. *Anim. Feed Sci. Technol.* **2021**, *276*, 114920. [[CrossRef](#)]
20. Xia, S.; Chen, L.; Liang, J. Enriched selenium and its effects on growth and biochemical composition in *Lactobacillus bulgaricus*. *J. Agric. Food Chem.* **2007**, *55*, 2413–2417. [[CrossRef](#)]
21. Morales, G.; Llorente, I.; Montesinos, E.; Moragrega, C. A model for predicting *Xanthomonas arboricola* pv. *pruni* growth as a function of temperature. *PLoS ONE* **2017**, *12*, e0177583. [[CrossRef](#)]
22. Fesharaki, P.J.; Nazari, P.; Shakibaie, M.; Rezaie, S.; Banoee, M.; Abdollahi, M.; Shahverdi, A.R. Biosynthesis of selenium nanoparticles using *Klebsiella pneumoniae* and their recovery by a simple sterilization process. *Braz. J. Microbiol.* **2010**, *41*, 461–466. [[CrossRef](#)]
23. Oberdörster, G.; Oberdörster, E.; Oberdörster, J. Nanotoxicology: An emerging discipline evolving from studies of ultrafine particles. *Environ. Health Perspect.* **2005**, *113*, 823–839. [[CrossRef](#)]
24. Jia, X.; Li, N.; Chen, J. A subchronic toxicity study of elemental Nano-Se in Sprague-Dawley rats. *Life Sci.* **2005**, *76*, 1989–2003. [[CrossRef](#)]
25. Kojouri, G.A.; Sadeghian, S.; Mohebbi, A.; Mokhber Dezfouli, M.R. The effects of oral consumption of selenium nanoparticles on chemotactic and respiratory burst activities of neutrophils in comparison with sodium selenite in sheep. *Biol. Trace Elem. Res.* **2012**, *146*, 160–166. [[CrossRef](#)]
26. Baltić, M.Ž.; Dokmanović Starčević, M.; Bašić, M.; Zenunović, A.; Ivanović, J.; Marković, R.; Janjić, J.; Mahmutović, H. Effects of selenium yeast level in diet on carcass and meat quality, tissue selenium distribution and glutathione peroxidase activity in ducks. *Anim. Feed Sci. Technol.* **2015**, *210*, 225–233. [[CrossRef](#)]
27. Han, D.S.; Batchelor, B.; Abdel-Wahab, A. XPS analysis of sorption of selenium(IV) and selenium(VI) to mackinawite (FeS). *Environ. Prog. Sustain. Energy* **2013**, *32*, 84–93. [[CrossRef](#)]
28. Al-Hagar, O.E.A.; Abol-Fotouh, D.; Abdelkhalek, E.S.; Abo Elsoud, M.M.; Sidkey, N.M. *Bacillus niabensis* OAB2: Outstanding bio-factory of selenium nanoparticles. *Mater. Chem. Phys.* **2021**, *273*, 125147. [[CrossRef](#)]

29. Tugarova, A.V.; Mamchenkova, P.V.; Khanadeev, V.A.; Kamnev, A.A. Selenite reduction by the rhizobacterium *Azospirillum brasilense*, synthesis of extracellular selenium nanoparticles and their characterization. *N. Biotechnol.* **2020**, *58*, 17–24. [[CrossRef](#)] [[PubMed](#)]
30. Piacenza, E.; Presentato, A.; Bardelli, M.; Lampis, S.; Vallini, G.; Turner, R.J. Influence of bacterial physiology on processing of selenite, biogenesis of nanomaterials and their thermodynamic stability. *Molecules* **2019**, *24*, 2532. [[CrossRef](#)]
31. Schröder, I.; Rech, S.; Krafft, T.; Macy, J.M. Purification and characterization of the selenate reductase from *Thauera selenatis*. *J. Biol. Chem.* **1997**, *272*, 23765–23768. [[CrossRef](#)]
32. Qiu, H.; Gao, S.; Hou, L.; Li, A.; Zhu, L.-q.; Dong, J.; Chen, F. Selenium-enriched *Bacillus subtilis* improves growth performance, antioxidant capacity, immune status, and gut health of broiler chickens. *Biol. Trace Elem. Res.* **2023**, *201*, 5756–5763. [[CrossRef](#)] [[PubMed](#)]
33. Dudonné, S.; Varin, T.V.; Anhê, F.F.; Dubé, P.; Roy, D.; Pilon, G.; Marette, A.; Levy, É.; Jacquot, C.; Urdaci, M. Modulatory effects of a cranberry extract co-supplementation with *Bacillus subtilis* CU1 probiotic on phenolic compounds bioavailability and gut microbiota composition in high-fat diet-fed mice. *Pharma Nutr.* **2015**, *3*, 89–100. [[CrossRef](#)]
34. Gan, F.; Hu, Z.; Huang, Y.; Xue, H.; Huang, D.; Qian, G.; Hu, J.; Chen, X.; Wang, T.; Huang, K. Overexpression of pig selenoprotein S blocks OTA-induced promotion of PCV2 replication by inhibiting oxidative stress and p38 phosphorylation in PK15 cells. *Oncotarget* **2016**, *7*, 20469. [[CrossRef](#)]
35. Pereira, F.C.; Wasmund, K.; Cobankovic, I.; Jehmlich, N.; Herbold, C.W.; Lee, K.S.; Sziranyi, B.; Vesely, C.; Decker, T.; Stocker, R. Rational design of a microbial consortium of mucosal sugar utilizers reduces *Clostridioides difficile* colonization. *Nat. Commun.* **2020**, *11*, 5104. [[CrossRef](#)]
36. Kasaikina, M.V.; Kravtsova, M.A.; Lee, B.C.; Seravalli, J.; Peterson, D.A.; Walter, J.; Legge, R.; Benson, A.K.; Hatfield, D.L.; Gladyshev, V.N. Dietary selenium affects host selenoproteome expression by influencing the gut microbiota. *FASEB J.* **2011**, *25*, 2492. [[CrossRef](#)] [[PubMed](#)]
37. Yang, J.; Wang, J.; Huang, K.; Liu, Q.; Liu, G.; Xu, X.; Zhang, H.; Zhu, M. Selenium-enriched *Bacillus subtilis* yb-114246 improved growth and immunity of broiler chickens through modified ileal bacterial composition. *Sci. Rep.* **2021**, *11*, 21690. [[CrossRef](#)] [[PubMed](#)]
38. Wu, Z. Transformation of Enriched Organic Selenium Lactic Acid Bacteria and Its Effects on Physiological and Rumen Flora of Tibetan Sheep. Master's Thesis, Xizang University, Linzhi, China, 2019. [[CrossRef](#)]

Disclaimer/Publisher's Note: The statements, opinions and data contained in all publications are solely those of the individual author(s) and contributor(s) and not of MDPI and/or the editor(s). MDPI and/or the editor(s) disclaim responsibility for any injury to people or property resulting from any ideas, methods, instructions or products referred to in the content.